Biophysical Journal, Volume *120*

Supplemental Information

Quantifying Intracellular Particle Flows by DIC Object Tracking

Anushree R. Chaphalkar, Yash K. Jawale, Dhruv Khatri, and Chaitanya A. Athale

SUPPORTING MATERIAL

Quantifying Intracellular Particle Flows by DIC Object Tracking (DICOT)

Anushree R. Chaphalkar, Yash K. Jawale, Dhruv Khatri and Chaitanya A. Athale*

Contents

1 Algorithm

The algorithm is described in Box **??**.

Algorithm 1 The routine describing image filtering using SoG and segmentation.

SoG

Image, Img $\leftarrow$ INPUT(filename)
Kernel-size, $k_{size} \leftarrow$ INPUT(int)
Kernel-spread, $\sigma \leftarrow$ INPUT(float)
ObjectType, $\lambda \leftarrow$ INPUT(bright=1,dark=-1)
Sensitivity, $\phi \leftarrow$ INPUT(float)
Strength of threshold, p $\leftarrow$ INPUT(int)
$h_G''(i,j) = e^{\frac{-(x^2+y^2)}{2\sigma^2}}$
$h_G(i,j) = \frac{h_G''(i,j)}{\sum_i^{k_{size}} \sum_j^{k_{size}} h_G''}$
$h'(i,j)_G = h_G - \langle h_G \rangle$
$h_{SoG} = \lambda \cdot h_G'(i,j) - \phi \langle h_G \rangle$
imFiltered $\leftarrow h_{SoG}(i,j) \circledast Img(n_1, n_2)$
Threshold, $\tau \leftarrow$ Otsu(imFiltered)

if imFiltered(j,k)> $\sqrt[p]{\tau}$ **then**
  imFiltered(j,k)$\leftarrow$ 1
else
  imFiltered(j,k) $\leftarrow$ 0
end if

2 Supplemental Tables

Sample	k_{size}	σ	λ	ϕ	p
E. coli [DIC]	11	3.25	1	0	3
E. coli [DAPI]	11	3.25	1	0	3
Beads [Phase]	5	1.75	0	0.01	1
MT [Rh]	15	1.25	1	0	1
Rice (edge)	3	1.25	1	0	1
Rice (blob)	11	2.5	1	0	0.97

Table S1: **Parameters of the SoG filter for varied samples.** The parameters input to the SoG filter for detecting objects in diverse imaging modes (DIC, phase contrast and fluorescence microscopy) are listed, with the outputs seen in Fig. **??**.

3 Supplemental Figures

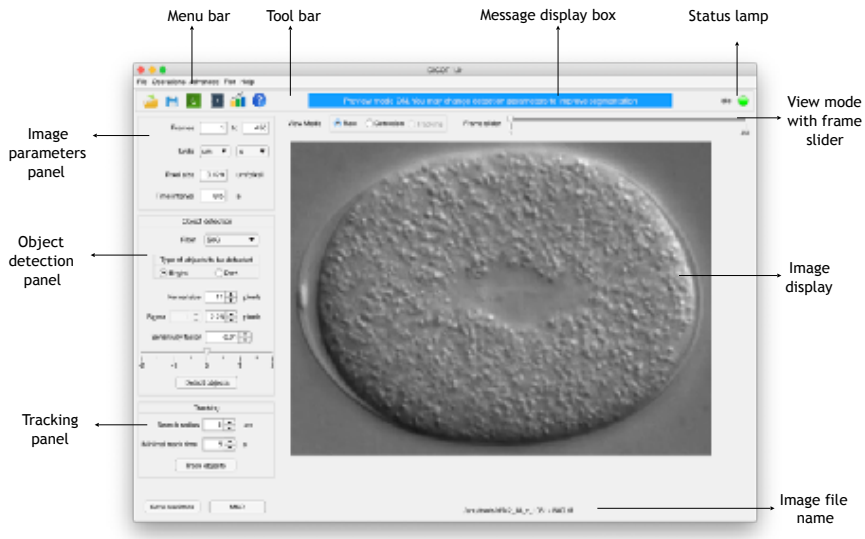

Figure S1: **GUI interface for the DIC object detection and tracking code.** The program has a GUI interface with a single pane. The menu bar can be used along with the icons to (i) select and parse the image data, (ii) detect objects and interactively view the results in the image-pane and (iii) the tracking panel to determine the criteria to track detected objects. The buttons on the very bottom export the statistics into text files as well as calculate mean square displacement (MSD) plots and fit the average curve either to an anomalous diffusion or diffusion and drift model. A detailed user guide is provided with the source code at `https://github.com/CyCelsLab/DICOT`.

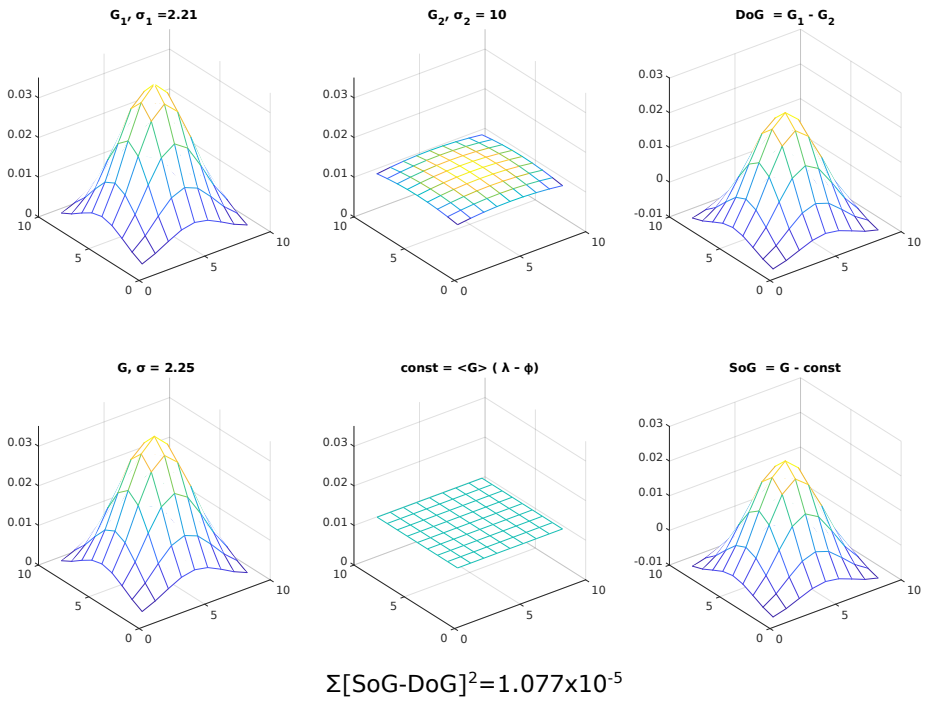

Figure S2: **The 2D profiles of comparable DoG and SoG filters.** *First row* A DoG filter is created by subtracting a Gaussian filter G_2 with $\sigma_2 = 10$ from G_1 with $\sigma_1 = 2.21$ to create a DoG filter that strongly resembles an *Second row* SoG filter. Here, the difference between a Gaussian with $\sigma = \sigma_1 = 2.5$ and a constant, the product of the mean of the Gaussian with $\lambda - \phi$ where $\lambda = 1$ is the switch parameter and $\phi = 0.01$ the sensitivity factor. The sum of square errors between these two functions is 1.07×10^{-5}.

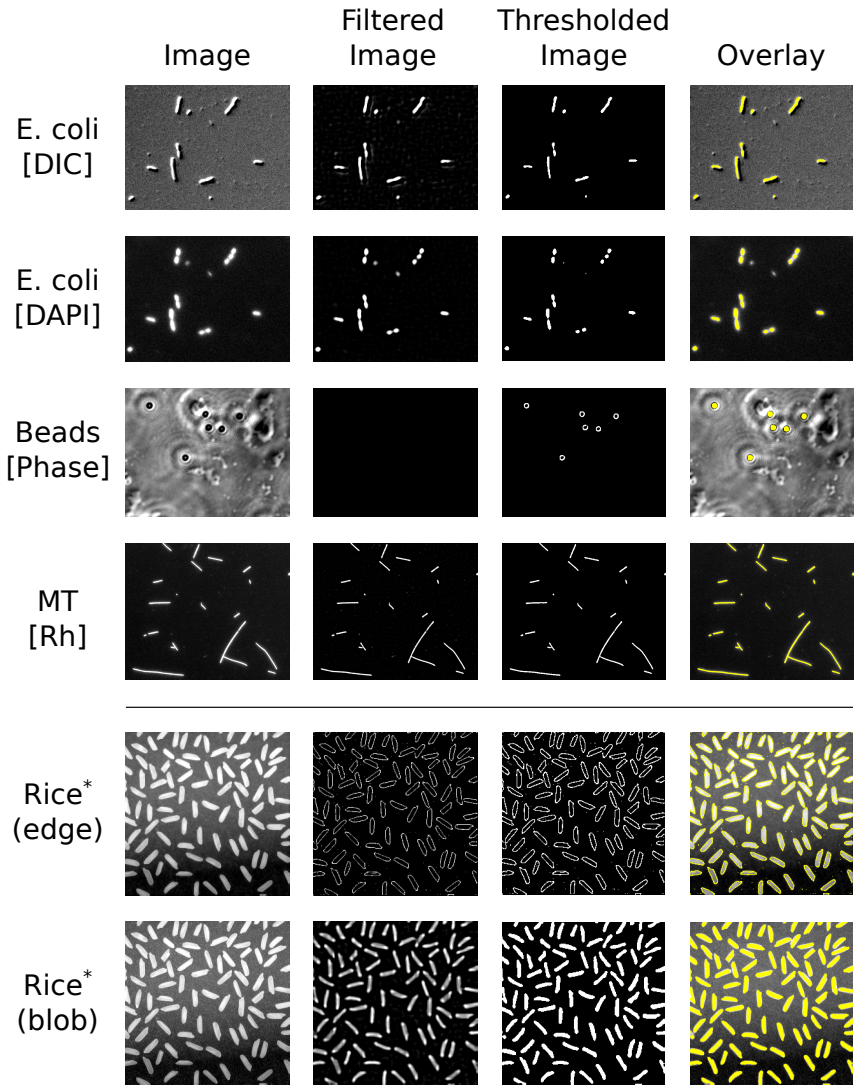

Figure S3: **SoG applied to diverse images.** Object detection from images acquired in different modes of microscopy was attempted by SoG filtering. (Top-Bottom) *Escherichia coli* cells in DIC, *E. coli* stained with DAPI in fluorescence, micron size beads in phase contrast microscopy (holes filled in threshold image before overlay), rhodamine labelled microtubules (MT) in fluorescence and rice grains (*MATLAB demo image) processed by either edge or blob-detection. DICOT parameters for each of the samples are listed in Table **??**.

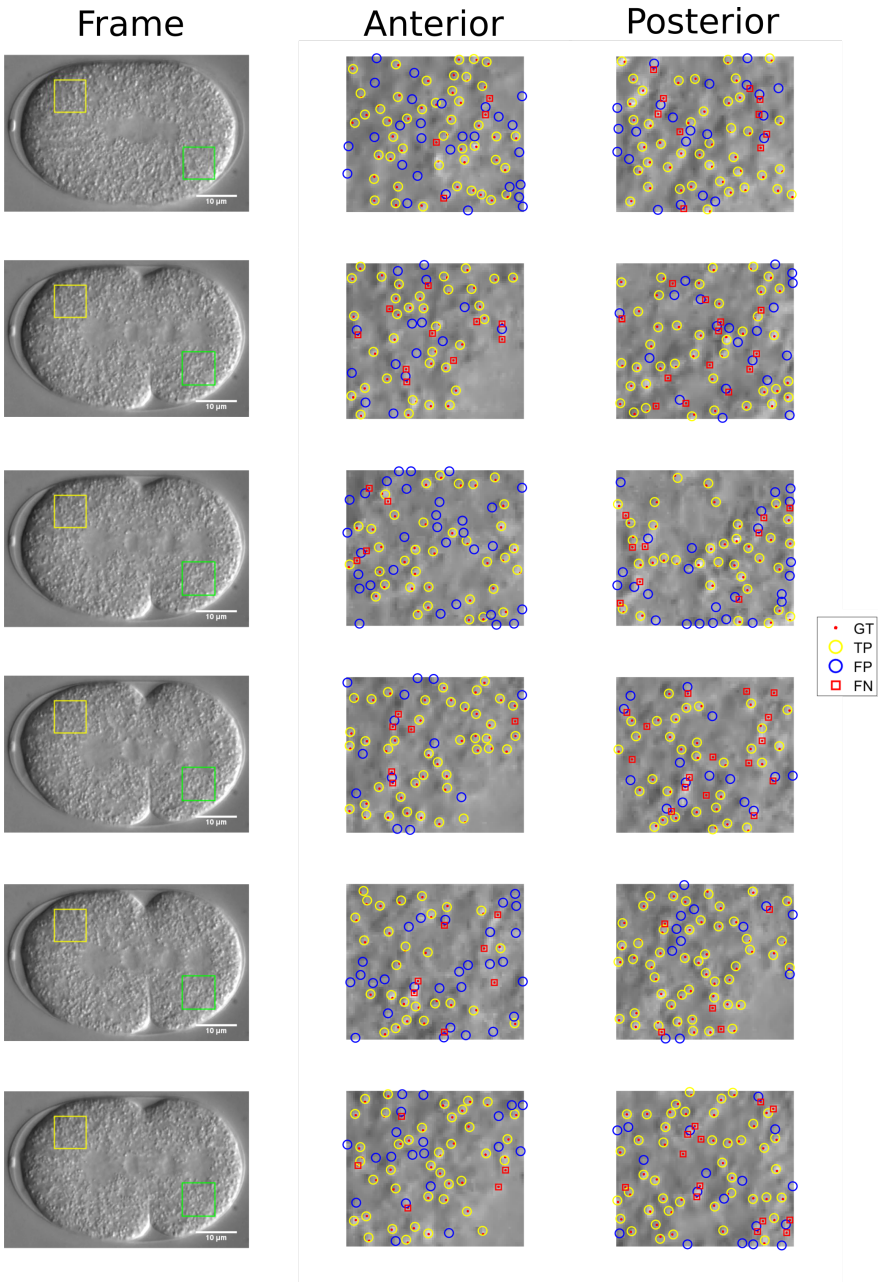

Figure S4: **Multiple ROIs used to evaluate object detection.** The *C.elegans* embryo time-series (N2_20_c_1001-1450) with frame numbers (*top to bottom*) 78, 295, 177, 335, 341, and 306 are overlaid with contour of regions of interest (ROIs) selected in anterior and posterior domains of the embryo. The representative panels from the anterior and posterior ROIs were manually annotated to mark lipid granules to serve as the ground truth GT (red dots) and after SoG image-filtering and segmentation used to determine true positives TP (blue circles), false positives FP (yellow circles) and false negatives FN (red squares), as described in the methods section. Scale bar 10 μm.

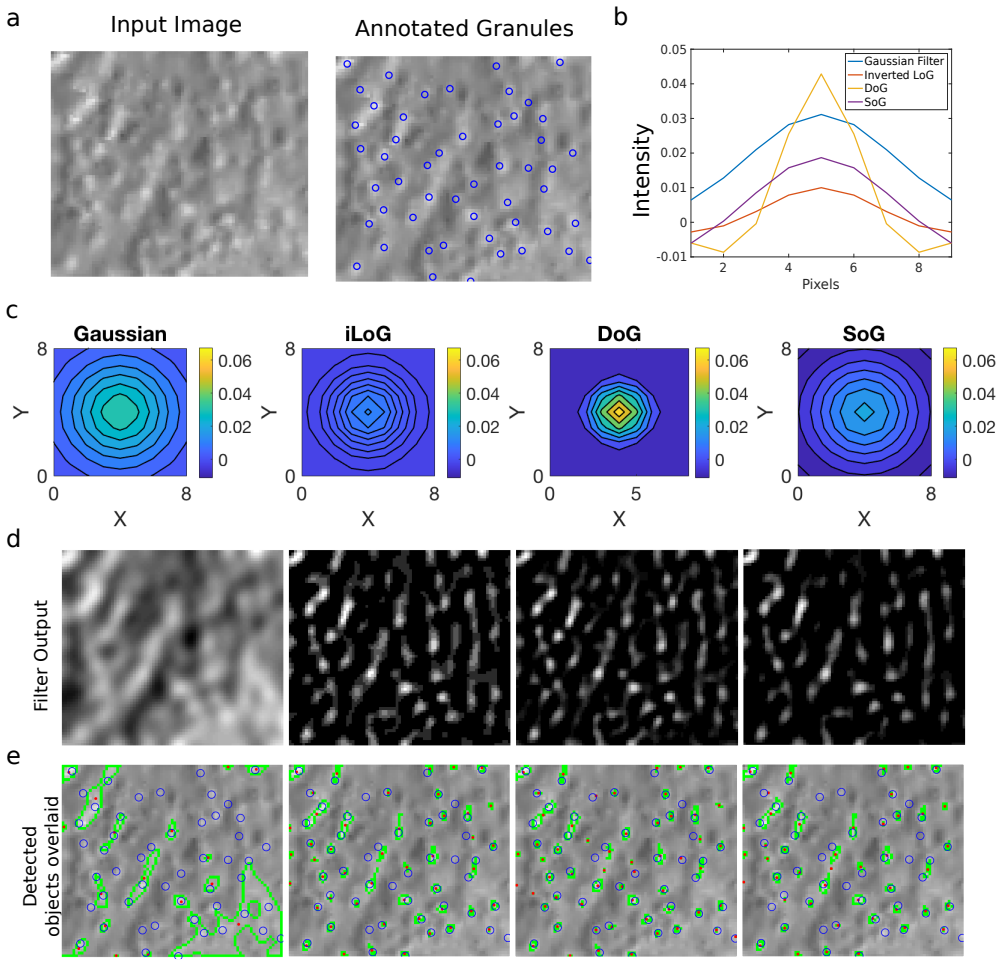

Figure S5: **Comparing filters for DIC object detection.** (a) An ROI from a mid-plane DIC image of a *C. elegans* embryo was manually annotated to mark lipid granules (blue circles). (b) Four different image filters were tested: Gaussian (blue), Inverted LoG (red), DoG (ochre) and SoG (purple). (c) Contour maps of multiple filters used to convolve the data are compared: Gaussian $\sigma = 2.25$, inverted Laplacian of Gaussian (iLoG) $\sigma = 2.25$, difference of Gaussian (DoG) taken between two functions with $\sigma = 1.25$ and 2.25 and Scaling of Gaussian (SoG) $\sigma = 2.25$. All filters have the same kernel size, i.e. 9 pixels. (c) The filtered output images (d) are then segmented by an automated threshold and the contours of detected objets (green) are used to estimate centroids (red dots) and compared to manual annotations (blue circles).

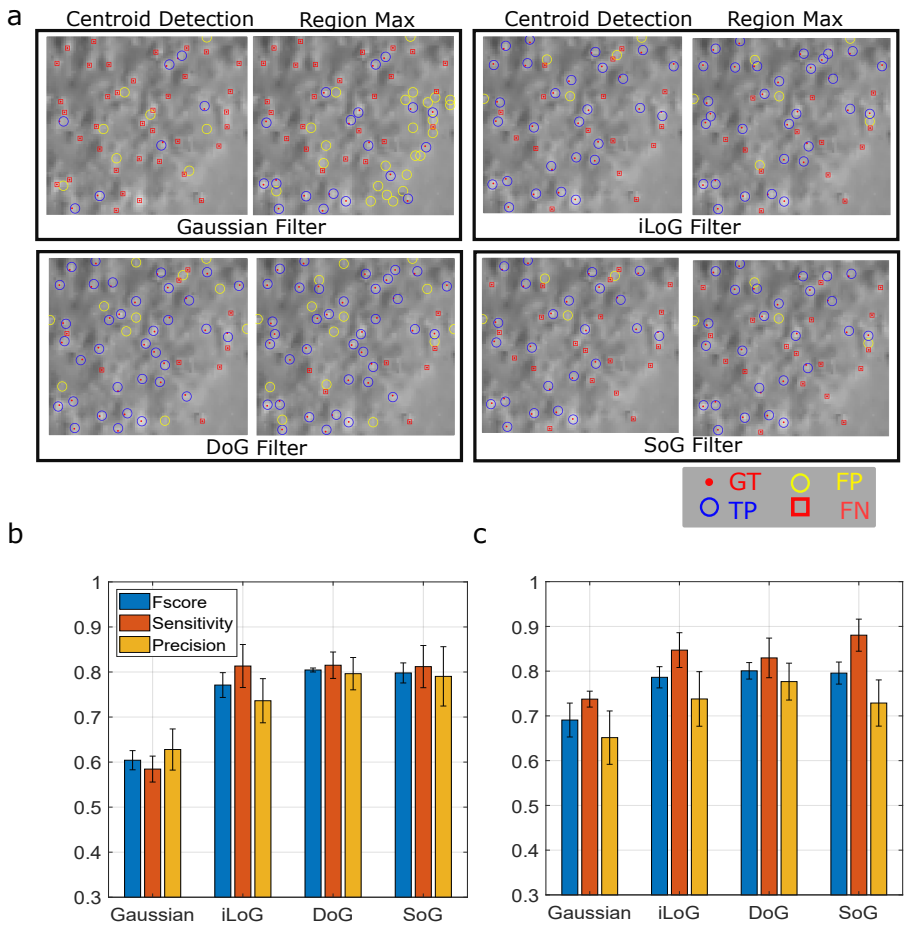

Figure S6: **Filters compared for sensitivity, precision and F1-score.** (a) An ROI from a mid-plane DIC image of a *C. elegans* embryo was manually annotated to mark lipid granules to serve as the ground truth GT (red dots) and compared to image-filtering with Gaussian, inverted Laplacian of Gaussian (iLOG), difference of Gaussian (DoG) and scaling of Gaussian (SoG). The respective true positives TP (blue circles), false positives FP (yellow circles) and false negatives FN (red squares) were determined as described in the methods section, comparing centroid and region-max based object detection. (b, c) The F-score, sensitivity and precision calculated from these comparisons for (b) centroids and (c) region-max based identification of objects are plotted.

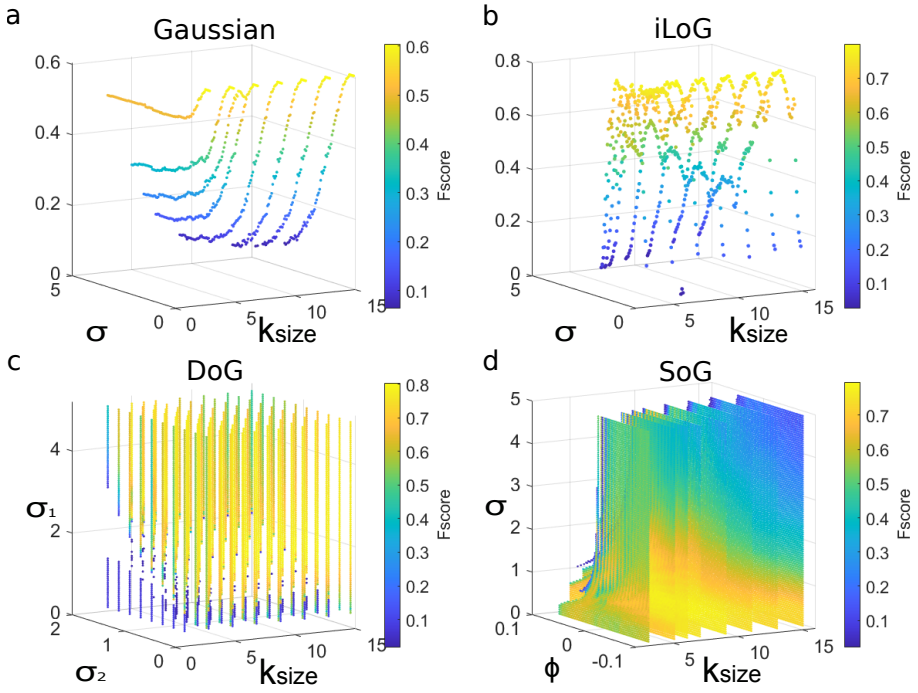

Figure S7: **Detection accuracy estimated by F1-score to compare filters.** (a) Gaussian, (b) inverted Laplacian of Gaussian (iLoG), (c) difference of Gaussian (DoG) and (d) scaling of Gaussian (SoG). For all filters the range of k_{size} was 3 to 15, σ was scanned over a range 0.1 to 5 with steps of 0.0495 while for DoG $\sigma_1 = \sigma$ while σ_2 was varied between 0.1 and 2 with steps of 0.211. For SoG the sensitivity factor ϕ was sampled between -0.1 and 0.1 with steps of 0.002. Colorbar indicates the F1-score.

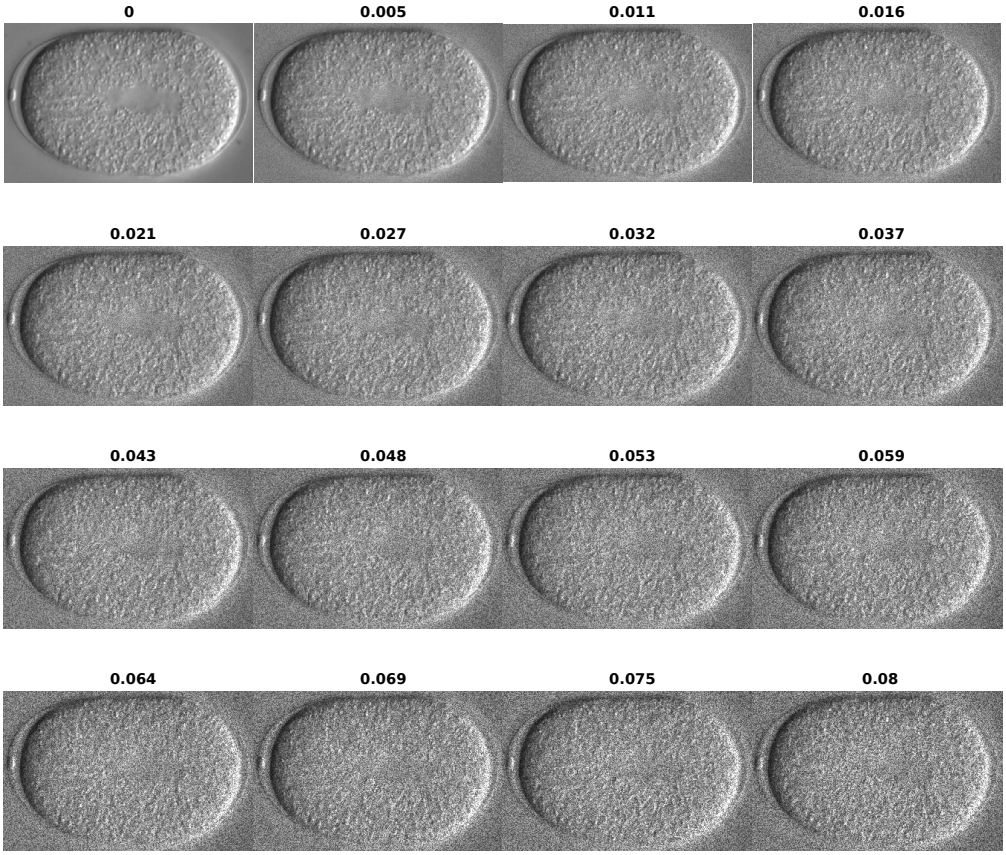

Figure S8: **Increasing noise of DIC image.** A single frame of a DIC image of *C. elegans* was subjected to increasing speckle noise with increasing variance of the noise ranging from 0 to 0.08. These images were used to test the error in positional detection using multiple filtering algorithms.

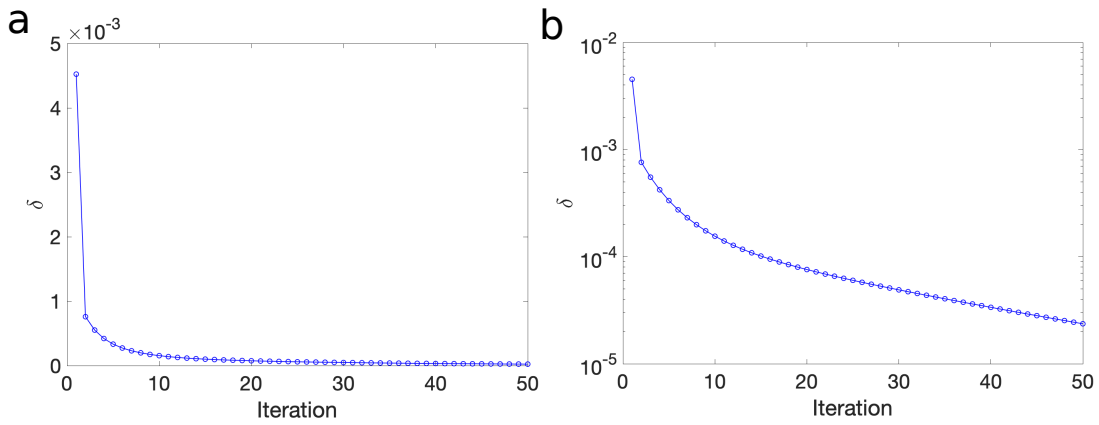

Figure S9: **Convergence of cost function to granule oscillations.** (a,b) The change of global deviation δ of the average curve to yolk granule oscillations (seen in Fig. 3(c)) are plotted on a (a) linear scale (b) semi-log scale.

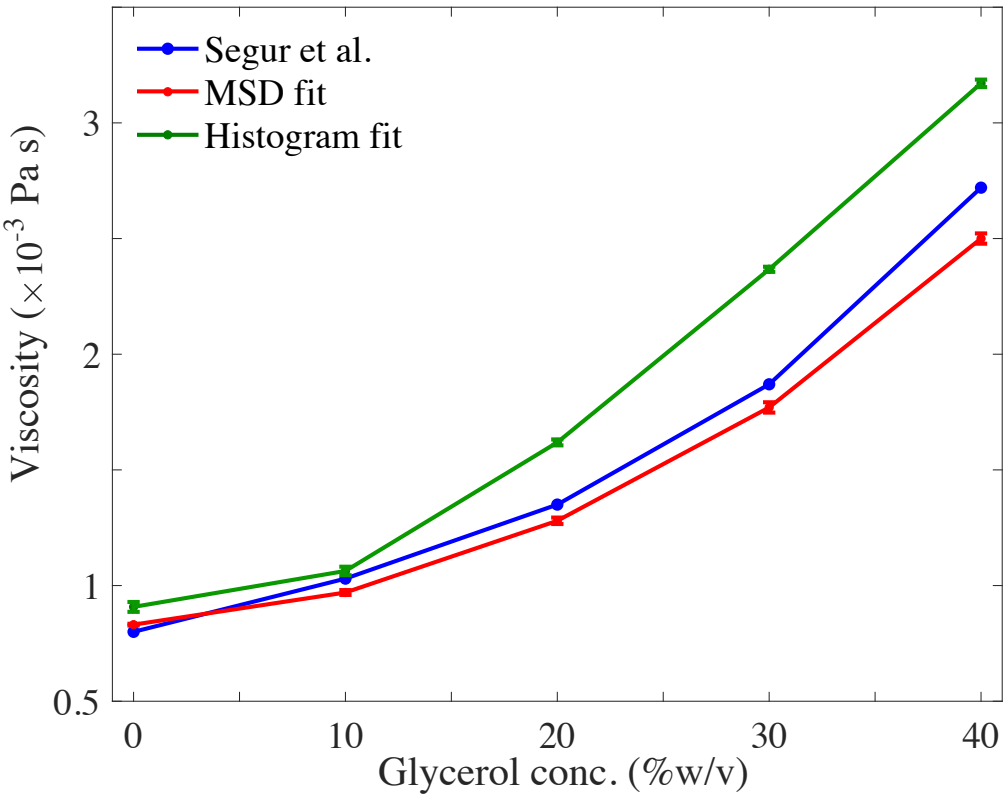

Figure S10: **Viscosity estimated using DICOT compared to literature.** The estimates of viscosity, η, obtained from tracking diffusing beads based on fitting the MSD (red) is compared to that using fits to the histogram of displacements (green). Both estimates are compared to bulk viscosity measurements of glycerol solutions [**?**]. All experimental estimates of η are mean±s.e.m. For n=10 fields of view.

4 Supplemental Videos

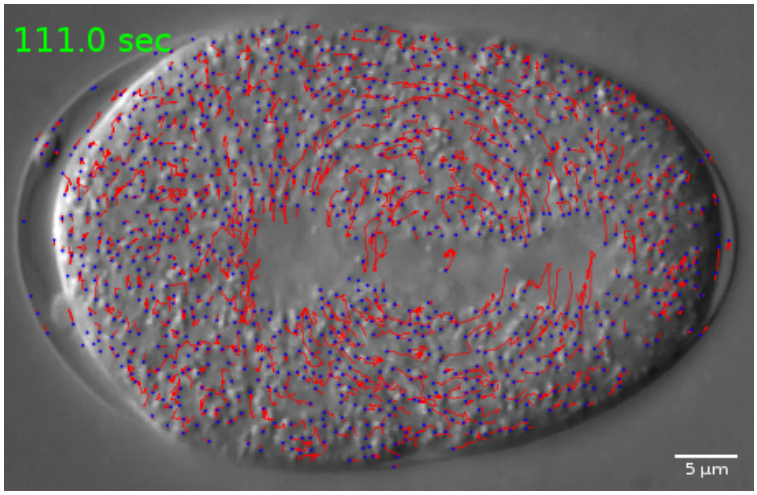

Video SV1: *C. elegans* **embryos with tracked granules.** The granules in a time series of *C.elegans* first embryonic division are tracked (blue dot - current position of granule, red line - trajectory of granules) using DIC tracking method. The time series have been described by Valfort et al. [**?**] (Image-Database). Scale: 5 μm; Δt: 0.5 s.

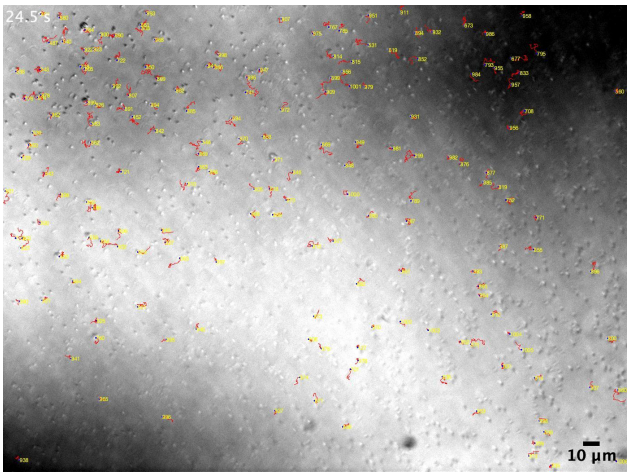

Video SV2: **Beads diffusing in water.** A representative time series of 1 μm beads diffusing in water tracked (blue dot - current position of granule, red line - trajectory of granules, yellow numbers - particle identifier) using SoG filter. Scale: 10 μm; Δt: 0.5 s

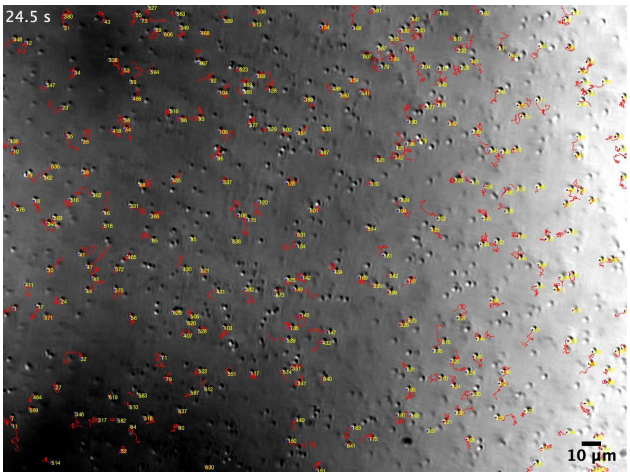

Video SV3: **Beads diffusing in 20% glycerol.** A representative time series of 1 μm beads diffusing in 20% (w/v) glycerol tracked (blue dot - current position of granule, red line - trajectory of granules, yellow numbers - particle identifier) using SoG filter. Scale: 10 μm; Δt: 0.5 s

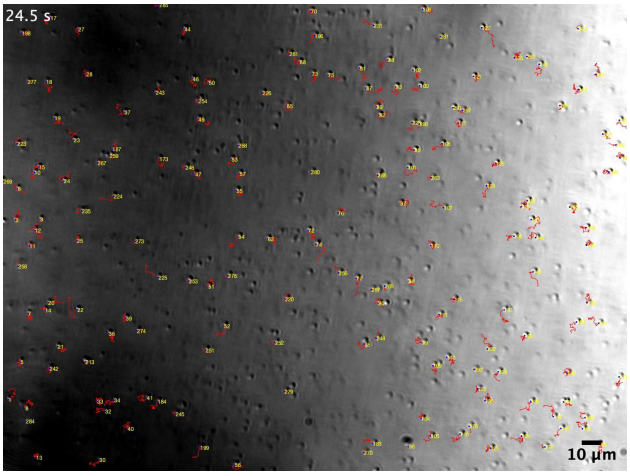

Video SV4: **Beads diffusing in 40% glycerol.** A representative time series of 1 μm beads diffusing in 40% (w/v) glycerol tracked (blue dot - current position of granule, red line - trajectory of granules, yellow numbers - particle identifier) using SoG filter. Scale: 10 μm; Δt: 0.5 s